

# Spatio-temporal Variability and Trends of Mean and Extreme Rainfall Events in the Sudano-sahelian Region of Cameroon

Ibrahim NJOUENWET (✉ [njouenwetibrahim@yahoo.fr](mailto:njouenwetibrahim@yahoo.fr))

University of Yaounde I: Universite de Yaounde I <https://orcid.org/0000-0003-1616-2226>

Lucie A. Djiotang Tchotchou

Universite de Yaounde 1 Faculte des Sciences

Brian Odhiambo Ayugi

Nanjing University of Science and Technology

Guy Merlin Guenang

Universite de Dschang Faculté des Sciences: Universite de Dschang Faculte des Sciences

Derbetini A. Vondou

Universite de Yaounde 1 Faculte des Sciences

Robert Nouayou

Universite de Yaounde 1 Faculte des Sciences

---

## Research Article

**Keywords:** Extreme precipitation indices, Sudano-sahelian regions, Precipitation, Irrigation, Food security

**Posted Date:** September 13th, 2021

**DOI:** <https://doi.org/10.21203/rs.3.rs-848441/v1>

**License:** © ⓘ This work is licensed under a Creative Commons Attribution 4.0 International License.

[Read Full License](#)

---

1 **Spatio-temporal variability and trends of mean and extreme rainfall events in the**  
2 **sudano-sahelian region of Cameroon**

3

4 **Ibrahim Njoudenwet\* · Lucie A. Djiotang Tchotchou · Brian Odhiambo Ayugi · Guy Merlin**  
5 **Guenang · Derbetini A. Vondou · Robert Nouayou**

6 **Received: date / Accepted: date**

7 Ibrahim Njoudenwet

8 Laboratory of Environmental Modeling and Atmospheric Physics, Department of Physics, University  
9 of Yaounde 1, P.O. Box 812 Yaoundé - Cameroon

10 Laboratoire Mixte International “Dynamique des écosystèmes continentaux d’Afrique Centrale en  
11 contexte de changements globaux” (LMI DYCOFAC), “Institut de Recherche pour le

12 Développement” (IRD, University of Yaoundé 1, IRGM), IRD P.O. Box 1857, Yaoundé, Cameroon

13 njoudenwetibrahim@yahoo.fr

14 <https://orcid.org/0000-0003-1616-2226>

15 Derbetini A. Vondou

16 Laboratory of Environmental Modeling and Atmospheric Physics, Department of Physics, University  
17 of Yaounde 1, P.O. Box 812 Yaoundé - Cameroon

18 Laboratoire Mixte International “Dynamique des écosystèmes continentaux d’Afrique Centrale en  
19 contexte de changements globaux” (LMI DYCOFAC), “Institut de Recherche pour le

20 Développement” (IRD, University of Yaoundé 1, IRGM), IRD P.O. Box 1857, Yaoundé, Cameroon

21 derbetini@yahoo.fr

22 <https://orcid.org/0000-0002-8681-5328>

23 Brian Odhiambo Ayugi

24 Jiangsu Key Laboratory of Atmospheric Environment Monitoring and Pollution Control,

25 Collaborative innovation Centre of Atmospheric Environment and Equipment Technology, School of

26 Environmental Science and Engineering, Nanjing University of Information Science and

27 Technology, Nanjing, 210044, China

28 ayugi.o@gmail.com

29 <https://orcid.org/0000-0003-3660-7755>

30 Guy Merlin Guenang

31 L2MPS, Department of Physics, Faculty of Science, University of Dschang, Dschang P.O. Box 96,  
32 Cameroon

33 merlin.guenang@yahoo.fr

34 Lucie A. Djiotang Tchotchou  
35 Laboratory of Environmental Modeling and Atmospheric Physics, Department of Physics, University  
36 of Yaounde 1, P.O. Box 812 Yaoundé - Cameroon  
37 angennes@yahoo.fr  
38 <https://orcid.org/0000-0003-2860-428X>

39 Robert Nouayou  
40 Laboratory of Geophysics and Geoexploration, Department of Physics, University of Yaounde 1,  
41 Cameroon  
42 rnouayou1@yahoo.fr

43 \*Correspondence to: Njouenwet Ibrahim (njouenwetibrahim@yahoo.fr )

44

45 **Abstract**

46 The Sudano-Sahelian region of Cameroon is mainly drained by the Benue, Chari and Logone rivers,  
47 which are very useful for water resources, especially for irrigation, hydropower generation, and  
48 navigation. Long-term changes in mean and extreme rainfall events in the region may be of crucial  
49 importance in understanding the impact of climate change. Daily and monthly rainfall data from  
50 twenty-five synoptic stations in the study area from 1980 to 2019 and extreme indices from the  
51 Expert Team on Climate Change Detection and Indices (ETCCDI) measurements were estimated  
52 using the non-parametric Modified Mann-Kendall test and the Sen slope estimator. The precipitation  
53 concentration index (PCI), the precipitation concentration degree (PCD), and the precipitation  
54 concentration period (PCP) were used to explore the spatio-temporal variations in the characteristics  
55 of rainfall concentrations. An increase in extreme rainfall events was observed, leading to an upward  
56 trend in mean annual. Trends in consecutive dry days (CDD) are significantly increasing in most  
57 parts of the study area. This could mean that the prevalence of drought risk is higher in the study  
58 area. Overall, the increase in annual rainfall could benefit the hydro-power sector, agricultural  
59 irrigation, the availability of potable water sources, and food security.

60 **Keywords:** Extreme precipitation indices, Sudano-sahelian regions, Precipitation, Irrigation, Food  
61 security

62

## 63 1- Introduction

64 The Sahelian region has been identified as the region with the highest rainfall variabilities in the  
65 world over the last century (Nicholson, 2000). Subsequently, it is presented as one of the world's  
66 largest semi-arid regions, where people's sources of income are mainly based on rain-fed agriculture  
67 and animal husbandry (Leisinger and Schmitt, 1995). However, Kharin et al., (2007) and Field  
68 (2012) have found that in the 21st-century climate change will negatively influence established  
69 resilience in the area, not only by increasing the year-to-year variability of rainfall patterns but also  
70 by also increasing unpredictable seasonality and an altered number of heavy rainfall events and  
71 droughts (Fischer et al., 2013; Taylor et al., 2017). The date of beginning and length of the dry and  
72 wet season and the amount of annual rainfall vary across the region (Niasse et al., 2004). However,  
73 agricultural crops are closely linked to factors such as water availability and seasonal parameters  
74 (onset and retreat date) (Berg et al., 2009; Sultan et al., 2005). Predominantly, the economies of West  
75 African countries including the Sahelian regions are directly affected through agriculture which is  
76 essentially rainfed, poor water quality, and poor management of water reservoirs for hydroelectric  
77 dams and irrigation (Niasse et al., 2004). However, data from stations in West Africa, and  
78 particularly the Sahel, are missing due to different policies in different countries (Sanogo et al,  
79 2015). For this reason, a review of the Intergovernmental Panel on Climate Change special report on  
80 extreme events (Field et al, 2012) highlighted the lack of studies on regional variability and trends in  
81 extreme rainfall and drought due to lack of data.

82 The sudano-sahelian region is the area's highest population density and also most vulnerable to  
83 climate change particularly, in the Cameroon region (Molua and Lambi, 2006). In terms of  
84 administration, it includes the far north and the northern regions and accounts for over one-fifth of  
85 Cameroon's total territory. The far north region has 74.3% of the population living below the poverty  
86 line (INS, 2015). Subsistence agriculture (rainfed, irrigated) accounts for 65% of the region's  
87 economic activity (DSCN, 2002). The sudano-sahelian region holds a strategically important  
88 position in Cameroon's economic development due to its vast area, water resources which is the  
89 major source of electricity by hydropower plants, high agricultural productive potential, and nomadic  
90 animal husbandry. The Benue and Logone-Chari Rivers are the main source of stream in the Sudano-  
91 Sahelian regions of Cameroon, which extend from the Adamawa region in the south through Nigeria  
92 to the Niger River in the west and from Lake Chad in the north to Chad and Central Africa republic  
93 in the south of the study area respectively. The Benue River also feeds the Lagdo Reservoir. Lagdo  
94 dam on the river Benue, with a useful capacity of close to 6 billion m<sup>3</sup>, is the only classical

95 multipurpose dam in Cameroon because it facilitates at the same time the hydro-electricity  
96 production with a capacity of 84 MW, irrigation of 80000 ha of plantation, and river regulation for  
97 navigation (Kamga 2001). Thus, the rainfall distribution caused by climate change may severely  
98 affect the water cycle, and food security in the sudano-sahelian region of Cameroon.

99 From September 1982 to 2000, the sudano-sahelian region of Cameroon has suffered climate  
100 extreme events such as drought causing considerable impacts on the country's environment, human  
101 activities, and economy (MINEPDED, 2016). For instance, the September 2012 floods in Maga and  
102 Yagoua resulted in many lives being lost while others were displaced, and the main hospital and  
103 other public infrastructures destroyed due to heavy rainfall (Igri et al, 2015; Igri et al, 2018). During  
104 the same year, a serious threat to food security was reported in more than half of the administrative  
105 units with more than 14000 hectares of crops such as; 12000 hectares of cotton (6% of cotton crop  
106 cultivated) and 12375 fruit plants destroyed (Ministry of Agriculture and Rural Development, 2012).  
107 Cheo et al. (2010) showed that water resources vary with the changing climatic condition and the  
108 severity of the impact varies from region to region. As such, local studies are essential to analyze the  
109 changes in precipitation extremes.

110 Several studies have been reported assessing the spatiotemporal trends in mean and extreme rainfall  
111 events across West Africa (Sanogo et al, 2015; Zhang et al, 2017; Barry et al, 2018) which includes  
112 the sudano-Sahelian regions due to global warming. Most of these studies observed an increasing  
113 trend in annual mean rainfall and extremes events during 1980-2010. Likewise, over Central Africa,  
114 Fotso-Nguemo et al (2018) projected the increased trends in heavy rainfall over sudano-sahelian of  
115 Cameroon by 2100. However, most of these studies are limited in their assessment to specific  
116 regions delimited by the lack of station data in West Africa especially the sudano-sahelian region of  
117 Cameroon. At the local scale, only one study has been conducted. Fita et al, (2016) have analyzed  
118 long terms trends in the mean and climate variability (only rainfall) over the study area and found  
119 that at the 95% level of confidence 10% of stations displayed statistically significant decreasing  
120 while 5% of stations showed statistically significant increasing using homogeneous monthly and  
121 annual rainfall database of twenty-five stations located in Northern Cameroon. As such on a local  
122 scale, this study is unique in terms of its use of station density, comprehensive assessment of trends  
123 and changes in rainfall, its variability, and extreme events.

124 Accordingly, the objectives of this study are to fill this gap of data and extends the work of Sanogo  
125 et al, (2015), Zhang et al, (2017) Barry et al, (2018) in the Sahel West Africa an in by performing a  
126 more comprehensive assessment of the spatial variability and trends in rainfall amounts and extremes  
127 using three decades of station data with stations distributed all over sudano-sahelian of Cameroon.

128 Such information is important for decision-makers and farmers to address climate change through  
129 sustainable adaptation strategies. The rest of this paper is organized as follows: section two describes  
130 study area, data and methods while section three presents results and discussion. Final section  
131 elucidates the conclusion of the study.

## 132 **2-Study area, data and method**

### 133 **2.1 Study area and data**

134 The Sudano-Sahelian region lies between 7°N to 13°N longitudes and 11.5°E to 16°E latitudes (Fig.  
135 1). It is a relatively flat topography. It has a drainage area of about 100,000 km<sup>2</sup> with a population of  
136 about 5,530,643 inhabitants. It is located in the north of Cameroon and covers two administrative  
137 regions (the Far North and North). The sudano-sahelian region has geostrategic importance as a  
138 source of water resources, a potential of hydropower, and is favorable to the livestock and growth of  
139 cotton, millet, sorghum, maize, rice, groundnuts and onions. All these crops are supervised by major  
140 companies such as "Société de Développement du Coton (SODECOTON)" and "Société  
141 d'Expansion et de Modernisation de la Riziculture dans la ville de Yagoua (SEMRY)". The climate  
142 of the study area can be broadly divided into two: the Sahelian and Sudanian zone located northward  
143 and southward of 9°N, respectively. Generally, the climate is under the influence of the  
144 thermodynamic properties of the African monsoon which brings rains between June-September in  
145 Sahelian zone and May-October in sudanian zone. Rainfall increases from the north toward the south  
146 between 328 mm and 1708 mm. This area is under the strong influence of humidity advected from  
147 the Atlantic Ocean and southwesterly flow (Penlap et al, 2004). The daily temperatures are usually  
148 between 25-34°C

149 Data sets used in this work are daily and monthly rainfall from 25 stations across the Sudano-  
150 Sahelian region of Cameroon for the 40-year period. This data set is collected by the support services  
151 of the SODECOTON. Their locations are shown in Fig. 1 and they are described in Table 1.

## 152 **2.2 -Method**

### 153 **2.2.1 - Statistical test of homogeneity**

154 Data homogeneity was first tested using the Standard Normal Homogeneity Test (SNHT) for a single  
155 break (Alexandersson, 1986), the Buishand range test (Buishand, 1982), the Pettitt test (Pettitt, 1979)  
156 and the Von Neumann ratio test (Von Neumann, 1941) at 1% significance level. Three of the four  
157 tests are used to determine the years of a break (location-specific tests) while the Von Neumann ratio  
158 test (not location specific) does not specify the year of rupture but rather a value that, when

159 compared with a threshold set in relation to the number of years used in the test, indicates whether  
 160 the null hypothesis is rejected or not. The analysis is based on four tests, including three possible  
 161 results which depend on the number of tests rejecting the null hypothesis (breakpoint); when there is  
 162 zero or one test that rejects this hypothesis (useful), two tests (doubtful) and three tests (suspect). The  
 163 test variable is the annual rainfall. In the following, when a station is labeled either useful or doubtful  
 164 it may be used for trend analysis and variability; while when she is labeled suspect, she lacks  
 165 credibility. Details on the description of these four methods can be found in Wijngaard et al, 2003.

### 166 2.2.2 Precipitation concentration index

167 The PCI is known as an indicator powerful of rainfall concentration, droughts or floods risk  
 168 prediction and soil erosivity for annual and seasonal scales (wet and dry seasons) (de Luis et al.  
 169 2011). PCI was calculated on the annual and seasonal scale for each climate station. The PCI for a  
 170 given station data series can be calculated as below,

$$171 \quad PCI_{annual} = \frac{\sum_{i=1}^{12} P_i^2}{(\sum_{i=1}^{12} P_i)^2} \times 100 \quad (1)$$

$$172 \quad PCI_{wet} = \frac{\sum_{i=1}^{nw} P_i^2}{(\sum_{i=1}^{nw} P_i)^2} \times \frac{100 \times nw}{12} \quad (2)$$

$$173 \quad PCI_{dry} = \frac{\sum_{i=1}^{nd} P_i^2}{(\sum_{i=1}^{nd} P_i)^2} \times \frac{100 \times nd}{12} \quad (3)$$

174 where  $P_i$  is the monthly amount of rainfall in month  $i$ , calculated for each climate station. The  
 175 seasonal  $PCI_{dry}$  and  $PCI_{wet}$  was computed on a seasonal scale based on the dry season from October-  
 176 May and the wet season from June-September;  $nw$  and  $nd$  represent, respectively, the number of  
 177 rainy and dry season months.

182 As defined in the classification range of PCI values, Oliver (1980) detailed as follows: the rate of  
 183 positive values of PCI which has  $\leq 10$  termed as a uniform distribution (i.e., low precipitation  
 184 concentration);  $PCI > 10 \leq 15$  refers moderate precipitation distribution;  $PCI > 16 \leq 20$  refers irregular  
 185 precipitation distribution, and  $PCI > 20$  describes strong irregularity of precipitation distribution.

### 186 2.2.2 Calculation of PCD and PCP

187 The PCD and PCP were proposed by Zhang and Qian (2003) to measure the distribution of rainfall  
 188 and the month in a year in which total precipitation concentrates respectively. They showed that the  
 189 length of the rainy season or the number of rainy days is inversely related to the PCD value. It is  
 190 developed based on the assumptions that the monthly total precipitation is a vector containing both  
 191 magnitudes. They can be defined as below:

$$192 \theta_j = \left( 360^\circ \times \frac{j}{n} \right) \quad (4)$$

$$193 R_i = \sum_{j=1}^N r_{ij} \quad (5)$$

$$194 R_{xi} = \sum_{j=1}^N r_{ij} \times \sin \theta_j \quad (6)$$

$$195 R_{yi} = \sum_{j=1}^N r_{ij} \times \cos \theta_j \quad (7)$$

$$196 PCD_i = \frac{\sqrt{R_{xi}^2 + R_{yi}^2}}{R_i} \quad (8)$$

$$197 \alpha_i = \tan^{-1} \left( \frac{R_{xi}}{R_{yi}} \right) \quad (9)$$

$$198 PCP_i = \alpha_i \times \left( \frac{n}{360} \right) \quad (10)$$

199 Where  $i$  is the year ( $i = 1980, 1981, \dots, 2012$ ), and  $R_i$  is the amount of rainfall of a year.  $j$  is the  
 200 month ( $j = 1, 2, \dots, 12$ ).  $\theta_j$  represents the corresponding azimuth angle of the  $j^{\text{th}}$  month, while the year  
 201 can be seen as  $360^\circ$ .  $R_{ij}$  represents the precipitation of the  $j^{\text{th}}$  month in the  $i^{\text{th}}$  year.

### 202 2.2.3 Precipitation Indices

203 Eleven indices of extreme precipitation defined by the Expert Team on Climate Change Detection  
 204 and Indices (ETCCDI) were considered (Zhang et al., 2011) and calculated using the R-climindex  
 205 model (Table 2).

### 206 2.2.4 The Modified Mann-Kendall trend tests

207 The Modified Mann-Kendall (MMK) trend test was applied respectively to examine trends in the  
 208 precipitation and the extreme precipitation indices and to identify trends from 1980 to 2012. These  
 209 methods are regularly used by researchers to separate natural variability of climate from  
 210 unidirectional climate change due to global warming (Shiru et al., 2019; Iqbal et al, 2019; Ayugi et  
 211 al., 2021; Ngoma et al., 2021). The classical Mann-Kendall test statistic ( $S$ ) for a time series,  $x$  with  $n$   
 212 number of data points can be computed as below (Mann, 1945; Kendall, 1975) :

$$S = \sum_{k=1}^{n-1} \sum_{j=i+1}^n \text{sgn}(x_j - x_i) \quad (11)$$

where

$$\text{sgn}(x_j - x_i) = \begin{cases} +1 & \text{if } (x_j - x_i) > 0 \\ 0 & \text{if } (x_j - x_i) = 0 \\ -1 & \text{if } (x_j - x_i) < 0 \end{cases}$$

The Mann-Kendall Z statistics are calculated from Eq. (12)

$$Z = \begin{cases} \frac{S-1}{\sqrt{\text{Var}(S)}} & \text{if } S > 0 \\ 0 & \text{if } S = 0 \\ \frac{S+1}{\sqrt{\text{Var}(S)}} & \text{if } S < 0 \end{cases} \quad (12)$$

where, Var (S) is the variance of S.

The significance of trend estimated by the use of MK test is first removed from the time series in MMK test (Rao and Hamed, 2008), then equivalent normal variants of rank ( $R_i$ ) of the detrended series is estimated as:

$$Z_i = \Phi^{-1} \left( \frac{R_i}{n+1} \right) \text{ for } i=1:n \quad (13)$$

where,  $\Phi^{-1}$  is the inverse standard normal distribution function. The self-similarity correlation matrix of the time series or the Hurst coefficient (H) is derived using the equation that defines as: (Koutsoyiannis, 2003):

$$C_n(H) = [\rho_{|j-i|}], \text{ for } i=1:n; j = 1:n \quad (14)$$

$$\rho_l = \frac{1}{2} (|l+1|^{2H} - 2|l|^{2H} + |l-1|^{2H}) \quad (15)$$

where,  $\rho_l$  is the autocorrelation function of lag l for a given H, and is computed by the use of maximum log likelihood function. The significance level of H is estimated by the use of mean and standard deviation for  $H = 0.5$ . If H is found significant, the biased estimate of the variance of S is calculated using the following equation for given H:

$$V(S)^{H'} = \sum_{i<j} \sum_{k<l} \frac{2}{\pi} \sin^{-1} \left( \frac{\rho_{|j-i|} - \rho_{|i-l|} - \rho_{|j-k|} - \rho_{|i-k|}}{\sqrt{(2-2\rho_{|i-j|})(2-2\rho_{|k-l|})}} \right) \quad (16)$$

The unbiased in estimation of  $V(S)^H$  is removed using a bias correction factor, B as below:

$$V(S)^H = V(S)^{H'} \times B \quad (17)$$

where, B is a function of H. The significance of MMK test is computed using Eq. (12) by replacing V (S) with  $V(S)^H$ . where the Z-statistics value exceeds the  $\pm 1.96$  level, indicating that the trend is

239 significant at the 95% significance level. The positive value of Z shows an increasing trend, while  
240 the negative value indicates a decreasing trend in the precipitation time series.

### 241 **2.2.5 Sen's slope estimator**

242 In this case, the true slope (change per unit time) was evaluated using a simple non-parametric  
243 procedure developed by Sen, (1968), which assumes that the trend is linear.

$$244 \text{ slope} = \text{median} \left( \frac{x_i - x_j}{i - j} \right) \quad (18)$$

245 where  $1 < i < j < n$  and  $n$  is the total number of the dataset.

### 246 **2.2.6 Standardized Precipitation Index**

247 The Standardized Precipitation Index (SPI) was calculated for each climate station and on the long-  
248 term precipitation record of the whole study area. The SPI values indicate the quantitative definition  
249 of drought conditions that could be computed for different time scales to investigate the variation of  
250 groundwater, surface water storage, and agriculture. In this study, 3-month and 12-month SPI were  
251 analyzed using monthly rainfall data for the assessment of drought intensity and susceptibility at  
252 seasonal and annual precipitation in the Sudano-Sahelian region of Cameroon. McKee et al. (1993)  
253 indicate that high positive values correspond to wet sequences and high negative values correspond  
254 to drought periods. The SPI values of -1.0 to -1.49, -1.5 to -1.99 and below -2.0 represent moderate,  
255 severe, and extreme droughts, respectively (McKee et al. 1993). It is also classified as the range of  
256 positive values of SPI which has above 2, 1.99 to 1.5, 1.49 to 1.0 and 0.99 to -0.99 design extremely  
257 wet, very wet condition, moderately wet and near-normal condition respectively.

### 258 **2.2.7 Spatial interpolation**

259 Mean and extreme rainfall are spatially represented using Kriging interpolation method.  
260 Geographical information system (GIS) in R software is used for this purpose. Studies show that  
261 Kriging gives better local interpolation than other methods in the Sudano-Sahelian of Cameroon  
262 (Djoufack et al, 2012; Dassou et al, 2016). Our focus here is given the lack of station observations  
263 and the GIS is used to fill gaps and show the spatial variability of precipitation and precipitation  
264 extremes.

## 265 **3. Results and discussions**

### 266 **3.1 Homogeneous assessment**

267 Few stations have missing values, with fewer than 4% (Table 1). Homogeneity results show that

268 72% of stations are labelled as “useful” as shown in Table 3. Fignole, Guetale, Hina-marbak,  
269 Touboro and Maroua stations were classified as “doubtful”. The Mora and Gawar stations are the  
270 only remaining stations and labelled “suspect”. After assessment of homogeneity, the Mora and  
271 Gawar stations were removed and data from 23 stations should be used for the analysis of trends and  
272 variability.

### 273 **3.2 Precipitation concentration index (PCI)**

274 The mean annual and seasonal PCI values are presented in Fig. 2a, b, and c. Fig. 2a shows complex  
275 spatial patterns of the annual average PCI values across the sudano-sahelian region, which varies  
276 from values lower than 20 in the south to higher than 25 in the far north-eastern. In addition, the  
277 lowest PCI values are observed in the southern part, ranging from 15 to 20 which is a characteristic  
278 of seasonality. While, in the central and far north part of the study area, ranging from 20 to 25  
279 suggests that these areas have a strong seasonal precipitation distribution throughout the year (Fig.  
280 2a). However, we detected a general increase in PCI values in most stations. Thus, significant  
281 increases and decreases in precipitation concentration values are found mainly in the Fignole and  
282 Maroua stations in the southern and northern part, respectively. This result indicates that the intra-  
283 annual distribution of rainfall is becoming less and less heterogeneous in the Sudano-Sahelian region  
284 and denotes heavy rainfall falling within a few months throughout the study period.

285 During the dry season, the spatial pattern demonstrated strong irregular rainfall distribution with PCI  
286 value  $> 20$  in the study area (Fig. 2(b)). For the wet season, rainfall was generally uniformly  
287 distributed over a 33-year period, analyzed having moderate concentration with  $PCI < 15$  as shown in  
288 Fig. 2(c). In general, similarly to PCI annual, the spatial map of seasonal PCI shows clear south  
289 (lower) to the north gradient (higher). Similar studies in regions such as Ethiopia, (Shawul, et al.,  
290 2020), Spain (de Luis et al., 2011) and China (Zhang et al., 2019) all point to the fact that seasonal  
291 variation associated with more precipitation has a lower PCI value and inversely.

### 292 **3.3 Variability of PCD and PCP**

293 Figures 3 (a) and (b) illustrate the spatial distributions of PCD and PCP values and trends,  
294 respectively, over the study area from 1980 to 2012. PCD values ranged from a minimum of 0.69 at  
295 Ndock in the south-eastern part to a maximum of 0.80 at Lara and Waza in the far north of  
296 Cameroon. The number of stations with increasing trends of PCD was greater than that of those with  
297 decreasing trends (13 vs. 4). Among the stations with increasing and decreasing trends, only two and  
298 one stations showed significant trends at 95 % level respectively. These stations were Touboro and  
299 Fignole and Maroua respectively, which are scattered over the southern and northern parts of the

300 study area. These results indicate that the annual precipitation in a year decreases from the southeast  
301 to the far north, implying a higher probability of flood events in a year toward the northeast than in  
302 other parts of the study area (Figures 3 (a)).

303 Mean PCP ranged from a minimum of 7.32 at Sanguere to a maximum of 7.52 at Doukoula et  
304 Ndock, which implies that annual rainfall mainly falls in July. The finding indicates that the wet  
305 season arrives earlier in the central regions of the study area. The spatial distributions of trend  
306 directions of PCP showed 19 stations out of 23 increasing trends, with only three sites (Touboro,  
307 Doukoula and Mokolo) being significant at 95 % level. This indicates that the rainy season exhibited  
308 a very slight temporal change in an increasing direction over the period 1980-2012, implying a  
309 slightly later occurrence of precipitation (Figures 3 (b)).

310 PCD and PCP are in good agreement with the results of many studies examining rainfall metrics in  
311 the wet season (onset and cessation of the wet season, number of rainy days) in and around Sahel  
312 regions. For example, Zhang et al, (2018) analyzed the spatial pattern of seasonal-rainfall metrics  
313 over the period 2000-2015. They found a clear north-south gradient was observed for the onset date  
314 and rainy days (RD). Another study is the one conducted by Sultan et al. (2010). They examined the  
315 climate-yields relationships in 28 administrative units in North-Cameroon. They found that the  
316 center of North-Cameroon is the most productive area and those with the wettest conditions in June.

### 317 **3.4 Annual rainfall analysis**

318 Temporal variability of annual rainfall in Sudano-Sahelian is shown in Table 4. Rainfall amounts for  
319 the period 1980-2012 displayed high spatial variability which is largely associated with the latitude  
320 variation within the study area. Low latitude regions received more precipitation than high latitude  
321 regions where the climate varies mainly from semi-arid to arid. In the low-latitude regions in the  
322 sudanian region, annual rainfall varied from 660.0 mm at Madingring station to 1708 mm at Ndock  
323 station while that in the high-latitude regions in the sahelian region of the study area varied from 329  
324 at Guider station to 1319 mm at Bidzar station. The temporal variability in the annual was assessed  
325 using the standard deviation of annual precipitation from the mean rainfall which showed a strong  
326 variation from 122.15 mm in the Sahelian region to 225.79 mm in the Sudanian region with the  
327 amount of rainfall received during that period. In order, the analysis of annual rainfall by Sen's slope  
328 method showed that most of the rainfall stations displayed upward trends.

329 Only Hina-Marbak, Kaélé, Bere, Garoua, Tchollire and Maroua stations, respectively found to have a  
330 statistically significant increasing trend at a rate of +7.0, 6.34, 3.52, 3.82, 10 and 10 mm/year of  
331 annual rainfall series as shown in Table 4. Most of the climate stations in the Sudano Sahelian region

332 have also exhibited an increasing trend of annual rainfall, although the trend is not significant.  
333 Similar findings were observed over the last three decades at the global level of West Africa (Barry  
334 et al, 2018; Chaney et al. 2014) and at a regional level of Sahel West Africa (Mouhamed Ly et al,  
335 2013; Sanogo et al, 2015).

### 336 **3.4 Annual maximum daily rainfall**

337 Among the parameters needed to calculate extreme precipitation is the maximum daily rainfall,  
338 which is commonly used to assess extreme conditions associated with flood risk (Westra et al. 2017,  
339 Field et al. 2012; Min et al. 2011). Fig. 4 shows the annual maximum daily (AMD) rainfall series  
340 analyzed for whole climate stations that are distributed in the Sudano-Sahelian zone of Cameroon  
341 from the year 1980 to 2012. The highest daily rainfall was obtained at Sanguere station which is  
342 found to be 184 mm in 1991, whereas the highest mean value of AMD rainfall of 92 mm was  
343 obtained at Tchollire station which is located near Adamawa plateau, and the lowest mean AMD  
344 value of 66.63 mm was recorded at Yagoua station in Northeastern part of the study area. The mean  
345 AMD rainfall corresponding to each weather station has shown a good correlation with latitude and  
346 annual rainfall which resulted in the Pearson correlation coefficient of -0.72 and 0.65 respectively.  
347 Fig. 4 provides more details on the periods and the return levels determined from GEV law. The  
348 highest AMD rainfall predicted over -10, -20, -50, and -100 years was obtained at the Tchollire  
349 station, with 129.55, 151.95, 182.46, 209.25 mm respectively. In order to predict the AMD rainfall,  
350 most sites showed non-significant increasing trends. Bidzar, Hina-Marbak, Kaele, Tchatibali, Bere,  
351 and Garoua stations exhibited significant increasing trends at rates of 0.84, 0.59, 3.62, 0.4, 0.5 and  
352 1.3 mm respectively, in Sudano-Sahelian of Cameroon. Among these stations, Leumbe et al, (2015)  
353 map the Maga zone located in the northeast of the study area, in which the Yagoua, Maroua and  
354 kaélé stations are subject to flood risks. This increase in extreme daily rainfall suggests an associated  
355 increase in intense Mesoscale Convective Systems (MCSs) in the Sudano-Sahelian region (Sanogo et  
356 al, 2015).

### 357 **3.6 Trend and magnitude of extreme precipitation events**

358 Zhang et al. (2011) classified the extreme precipitations into three groups: (1) intensity indices (mm):  
359 annual total wet-day precipitation (PRCPTOT), very wet days (R95p), extremely wet days (R99p),  
360 highest 1-day precipitation in a year (Rx1d), highest 5-day precipitation in a year (Rx5d) and simple  
361 daily intensity index (SDII, mm/day); (2) frequency indices (days): number of heavy precipitation  
362 days (R10mm), number of very heavy precipitation days (R20mm) and number of very heavy  
363 precipitation days (R25mm) and, (3) duration indices (days): consecutive dry days (CDD) and

364 consecutive wet days (CWD).

365 The spatial annual value and trends of duration and intensity indices from 1980 to 2012 over the  
366 Sudano-Sahelian are presented in Fig. 5. On average, stations in the northeast had the highest CDD  
367 values in the range 180-190 days, while stations in the southeast had the lowest in the range 150-160  
368 days. The trend in CDD is not significant. Subsequently, the CDD trend increased in most (southern  
369 and central parts) of the study area and significantly at a rate of 1.07, 0.6, 1.00 and 0.7 days/year in  
370 Fignole, Touboro, Bere, and Garoua stations, respectively. While insignificant negative trends are  
371 observed in the northern part of the study area (Fig. 5a). However, the opposite mean and no trend  
372 were noticed in CWD at most of the stations where the only significant decreasing trend was  
373 observed in the Fignole station at -0.05 days/year (Fig. 5b). Based on the spatial distribution of mean  
374 SDII values decreasing from south to north, the general trend is increasing at almost all of the  
375 stations with significant stations such as Hina-Marbak, Thollire, Pitoa, Lara, Soudounkou, Fignole  
376 and Touboro located in the northeast, central, southwest and southeast of the study area as shown in  
377 Fig 5f. For the indices representing the number of days of extreme rainfall, maps R10, R20 and R25  
378 showed a spatial pattern almost similar to SDII. In general, increasing trends can be observed with  
379 the only significant trend detected at Touboro and Tchollire at 0.25 and 0.4 days/year and negative at  
380 Sanguere at -0.16 days/year for R10 (Fig 5c). R20 showed a significant only upward and decreasing  
381 trend in Tchollire and Touboro and Doukoula stations, respectively (Fig 5d). R25mm values indicate  
382 significant increasing trends at Hina-marbak, Touboro, Bere and Tchollire stations.

383 As shown in Fig. 6, intensity indices displayed increasing trends, on average, during 1980-2012. A  
384 clear north-south gradient was observed for PRCPTOT, R95P, R99P, Rx1day, and Rx5day based on  
385 a 33-year (1980-2012) average value. From Fig. 6(a), it can be seen that PTOT increased in the study  
386 region. The increase was more evident at the Guidiguiss, Hina-Marbak, Soudounkou, Sanguere,  
387 Touboro, Tchollire and Ndock stations, distributed over the entire study area. Meanwhile, At the  
388 same time, a general increasing trend of R95p was observed with the significant stations being Hina-  
389 marbak, Garoua, and Touboro (Fig. 6(b)). Spatially, no trend was noticed in R99p at any of the  
390 stations (Fig. 6(c)).

391 The Pitoa, Bere, Garoua, Madingring and Doukoula regions appear to have experienced a significant  
392 increase at a rate of  $> 0.5$  mm/year with Rx1day (Fig. (6d)). whereas a significant increase of  $> 0.9$   
393 mm/year can be observed in Rx5day in the Hina-Marbak, Bere, Tchollire, Doukoula, Maroua and  
394 Lara regions, distributed over the central and southeastern parts of the study area (Fig. (6e)). Thus,  
395 the strong wetness of the Sahel is manifested both by more humid days but also by heavier extreme  
396 rainfall.

397 Pearson's product-moment correlation (CC) shows a positive correlation between annual PRCPTOT  
398 and other indices as shown in Table 5. The most extreme rainfall indices correlations except CDD  
399 and CWD were positive and significant at least 95 % confidence level. PRCPTOT is strongly  
400 correlated with R10mm, R20mm, R25mm, R95p, R99p, Rx1day and Rx5day values with CC of  
401 0.94, 0.92, 0.89, 0.75, 0.62, 0.58, 0.64, respectively. These extreme precipitation indices translate the  
402 positive change in PRCPTOT while CDD and CWD negatively correlated; because CDD and CWD  
403 are an indicator of dry climate extremes. At the same time, all extreme maximum precipitation  
404 indices such as SDII are also significant among themselves. Globally, the CC values of extreme  
405 precipitation indices indicate that the study area with lower and higher mean annual precipitation can  
406 produce higher extreme precipitation values.

407 In accordance with the current findings, de Vondou et al. (2021) have also indicated that extreme  
408 rainfall indices represent patterns approximately similar to that of annual rainfall except CDD where  
409 the spatial south-north gradient is reversed. All extreme rainfall indices (except CWD), generally,  
410 increased in the sudano-Sahelian region of Cameroon during 1980-2012. Results are almost  
411 consistent with results obtained in previous studies at the regional level in West Africa (Barry et al.,  
412 2018; Sanogo et al., 2015), Central Africa (Aguilar et al., 2009) in the Sahelian region (Mouhamed  
413 Ly et al., 2013; Zhang et al., 2017), in some nearby areas, for example, Nigeria (Gbode et al., 2019).  
414 Several studies have justified the increasing rainfall trend over the last three decades by a recovery  
415 from the 1970-1980 droughts in West Africa in general (Druyan et al, et 2011; Chaney et al., 2014;  
416 Sanogo et al., 2015). In the same direction, Ibrahim et al (2014) in a further study reports both an  
417 increase in total annual rainfall and in the frequency of rainy days, which contributes to partial  
418 rainfall recovery in the Sahel. More recently, Globe et al. (2019) demonstrated that this recovery is  
419 summarized by a greater number of rainy days associated with a longer duration of the wet period  
420 and more extreme rainfall events. This was justified in the central-eastern Sahel in West Africa by  
421 the increase in vertical moisture flux, which is mainly driven by the increasing convergence of  
422 moisture from remote sources (Akinsanola and Zhou, 2018).

### 423 **3.7 Standardized precipitation index**

424 The Standardized Precipitation Index (SPI) is an index that indicates the standard deviations from the  
425 mean values for which an event occurs (Guenang et al, 2014). The fitted gamma distribution is used  
426 to calculate this index. The 3- and 12-month SPI were used to estimate the agricultural applications  
427 and groundwater storage variation (hydrological drought) of the Sudano-Sahelian of Cameroon  
428 based on long-term monthly precipitation data (1980-2019). Fig. 7 and 8 show the SPI values of 3-  
429 and 12-month time scales from 1980 to 2019. In addition, almost all stations exhibited the severe and

430 extreme droughts in the 1980s and 2010s while the 1990s were characterized by moderately wet  
431 moisture conditions. Thus, the analysis of SPI-3 and SPI-12 in this area present a severe hazard of  
432 drought for agriculture and groundwater storage. Njouenwet et al. (2021) have also concluded that  
433 the Sudano-Sahelian area of Cameroon exhibits the very high agricultural drought hazard zones,  
434 especially, where the maize and peanut grain crops are concerned. As found by Cheo et al (2013),  
435 variability results from an SPI-12 show that the wetter period surpasses the drier period in all  
436 regions. Mainly, the mid-1990s point out the climate shift in all stations as shown in Fig. 8.  
437 Following this, we observe similarities in the trends of SPI-12 at the different stations with the  
438 annual rainfall in the Sudano-Sahelian region, which corroborated those obtained by Sanogo et al,  
439 (2015) and Globe et al (2019).

#### 440 **4 Potential impacts of climate variability and extreme precipitation on agriculture and water** 441 **management**

442 Overall, the Sudano-Sahelian region of Cameroon from 1980 to 2012 recorded significant upward  
443 trends in annual rainfall and PRCPTOT index in our analysis, such as their interannual variability.  
444 They are related to the increase in extreme rainfall days. Rainfall during the rainy season is almost  
445 uniform, with low PCI levels and low risk of crop failure, but the amount and distribution of rainfall  
446 during this period with late rainfall onset dates have an impact on some crops and varieties, and thus  
447 on crop production and productivity. For instance, Sultan et al, (2009) found that the rainfall  
448 parameters (rainy season onset and length) are major drivers for the year-to-year and their variability  
449 impacts crop productivity. In addition, heavy rainfall can negatively impact crop yields and cause  
450 increased soil erosion. As mentioned in the introduction, the floods of September 2012 in Maga and  
451 Yagoua during which more than 14000 hectares of crops and 12375 fruit plants were destroyed  
452 (Ministry of Agriculture and Rural Development, 2012).

453 However, the study area is mainly drained by four streams which are Benue, Chari, Faro, and  
454 Logone. They extend to Chad, Nigeria, and RCA. Hence, the high value and increasing trends in  
455 annual PCI are observed over the same time period throughout the study area and could cause a  
456 challenge for water resource management. Increasing rainfall could favor hydropower production  
457 around the Lagdo dam and increase the supply of drinking water for industrial and domestic uses in  
458 the study area. Nevertheless, an increase in daily extreme precipitation (R1xday, R5xday, R95p, and  
459 R99p) indices could potentially lead to a greater probability of flooding. From 2010 to 2012,  
460 disastrous floods occurred in Yagoua and Guirvidig in the south-eastern part of the study area, as in  
461 many Sahelian countries, resulting in the destruction of the dyke, many deaths and material losses  
462 (Leumbe et al, 2015; Frédéric et al, 2020). On the other hand, as an indicator of lack of rainfall, an

463 increase in CDD and a decrease in CWD could create challenging situations for agricultural  
464 practices, food security, and runoff from major rivers.

## 465 **5 Conclusions**

466 This study analyzed spatio-temporal variability and changes in mean rainfall and extreme indices in  
467 the sudano-sahelian region of Cameroon based on daily synoptic rainfall datasets for the period from  
468 1980 to 2012. A homogeneity test was performed on the data series using the standard normal  
469 homogeneity test (SNHT), the Pettitt test, the Buishand range test, and the Von Neumann ratio test.  
470 The ETCCDI (Expert Team on Climate Change Detection Indices) indices were calculated using  
471 RClmDex version 1.0 software. These climate indices were used to assess corresponding trends in  
472 the frequency and intensity of daily rainfall and changes in the length of the season. Based on the  
473 Sen slope and Modified Mann-Kendall (MMK) trend test, most of the rainfall stations showed a  
474 statistically insignificant upward trend for annual rainfall. The temporal and spatial variability of  
475 precipitation using the Precipitation Concentration Index (PCI) and Precipitation Concentration  
476 Period (PCP) showed a higher variability of precipitation on the annual and dry season scale than the  
477 wet seasons. Most stations show increasing trends in the number of very heavy rains and  
478 precipitation intensity indices, so very few are significant. In addition, non-significant increasing and  
479 decreasing trends were observed in the south and north, respectively, for consecutive dry days  
480 (CDD) in the study area while the opposite trends were observed for consecutive wet days (CWD).  
481 However, this study highlights further research on how the hydrological regime responds to climate  
482 change causing flooding, food insecurity, and affecting water resources in the Sudano-Sahelian  
483 zones. It is beneficial for the future social and economic planning of the country and the sub-region.

## 484 **Acknowledgments**

485 The authors are grateful to SODECOTON's support department for providing the data for this study.  
486 This work is conducted within the framework of the research of the International Joint Laboratory  
487 "Dynamics of Terrestrial Ecosystems in Central Africa: A context of Global Changes" (IJL  
488 DYCOCA/LMI DYCOFAC). The authors acknowledge the helpful inputs of Franck Eitel  
489 KEMGAMG GHOMSI.

## 490 **Conflict of interest**

491 The authors declare that they have no conflict of interest.

## 492 **Funding Statement**

493 No funding was received for conducting this study.

#### 494 **Author's Contribution**

495 All authors contributed to the study conception and design. Ibrahim Njouenwet, Lucie A. Djiotang  
496 Tchotchou, Brian Odhiambo Ayugi, Guy Merlin Guenang, Derbetini A. Vondou and Robert  
497 Nouayou contributed to the conceptualization of the study. The first draft of the manuscript was  
498 written by Ibrahim Njouenwet and all authors commented on previous versions of the manuscript.  
499 All authors read and approved the final manuscript.

500

501

#### **References**

- 502 1. Aguilar, E., Barry, A. A., Brunet, M., Ekan, L., Fernandes, A., Massoukina, M., . . . Zhang,  
503 X. (2009). Changes in temperature and precipitation extremes in western central Africa,  
504 Guinea Conakry, and Zimbabwe, 1955–2006. *Journal of Geophysical Research*, *114*(D2).  
505 doi:10.1029/2008jd011010
- 506 2. Ajjur, S. B., & Riffi, M. I. (2020). Analysis of the observed trends in daily extreme  
507 precipitation indices in Gaza Strip during 1974–2016. *International Journal of Climatology*.  
508 doi:10.1002/joc.6576
- 509 3. Akinsanola, A. A., & Zhou, W. (2018). Dynamic and thermodynamic factors controlling  
510 increasing summer monsoon rainfall over the West African Sahel. *Climate Dynamics*, *52*(7-  
511 8), 4501-4514. doi:10.1007/s00382-018-4394-x
- 512 4. Akinsanola, A. A., & Ogunjobi, K. O. (2015). Recent homogeneity analysis and long-term  
513 spatio-temporal rainfall trends in Nigeria. *Theoretical and Applied Climatology*, *128*(1-2),  
514 275-289. doi:10.1007/s00704-015-1701-x
- 515 5. Alexandersson, H. (1986). A homogeneity test applied to precipitation data. *Journal of*  
516 *Climatology*, *6*(6), 661-675. doi:10.1002/joc.3370060607
- 517 6. Ayugi, B., Jiang, V., Zhu, H., Ngoma, H., Babaousmail, H., Karim, R., 2021. Comparison of  
518 CMIP6 and CMIP5 models in simulating mean and extreme precipitation over East Africa.  
519 *Int. J. Climatol.* <https://doi.org/10.1002/joc.7207>
- 520 7. Barry, A. A., Caesar, J., Tank, A. M., Aguilar, E., Mcsweeney, C., Cyrille, A. M., . . .  
521 Laogbessi, E. T. (2018). West Africa climate extremes and climate change indices.  
522 *International Journal of Climatology*, *38*. doi:10.1002/joc.5420
- 523 8. Berg, A., Quirion, P., & Sultan, B. (2009). Weather-Index Drought Insurance in Burkina-  
524 Faso: Assessment of Its Potential Interest to Farmers. *Weather, Climate, and Society*, *1*(1),  
525 71-84. doi:10.1175/2009wcas1008.1
- 526 9. Bhatti, A. S., Wang, G., Ullah, W., Ullah, S., Hagan, D. F., Noon, I. K., . . . Ullah, I. (2020).

- 527 Trend in Extreme Precipitation Indices Based on Long Term In Situ Precipitation Records  
528 over Pakistan. *Water*, 12(3), 797. doi:10.3390/w12030797
- 529 10. Buishand, T. (1982). Some methods for testing the homogeneity of rainfall records. *Journal*  
530 *of Hydrology*, 58(1-2), 11-27. doi:10.1016/0022-1694(82)90066-x
- 531 11. Chaney, N. W., Sheffield, J., Villarini, G., & Wood, E. F. (2014). Development of a High-  
532 Resolution Gridded Daily Meteorological Dataset over Sub-Saharan Africa: Spatial Analysis  
533 of Trends in Climate Extremes. *Journal of Climate*, 27(15), 5815-5835. doi:10.1175/jcli-d-  
534 13-00423.1
- 535 12. Cheo, A. E., Voigt, H., & Mbua, R. L. (2013). Vulnerability of water resources in northern  
536 Cameroon in the context of climate change. *Environmental Earth Sciences*, 70(3), 1211-  
537 1217. doi :10.1007/s12665-012-2207-9
- 538 13. Dassou, E. F., Ombolo, A., Chouto, S., Mboudou, G. E., Essi, J. M., & Bineli, E. (2016).  
539 Trends and Geostatistical Interpolation of Spatio-Temporal Variability of Precipitation in  
540 Northern Cameroon. *American Journal of Climate Change*, 05(02), 229-244. doi  
541 :10.4236/ajcc.2016.52020
- 542 14. Djoufack, V., Fontaine, B., Martiny, N., & Tsalefac, M. (2012). Climatic and demographic  
543 determinants of vegetation cover in northern Cameroon. *International Journal of Remote*  
544 *Sensing*, 33(21), 6904-6926. doi:10.1080/01431161.2012.693968
- 545 15. Druyan, L. M. (2010). Studies of 21st-century precipitation trends over West Africa.  
546 *International Journal of Climatology*, 31(10), 1415-1424. doi :10.1002/joc.2180
- 547 16. DSCN. (2002) - Conditions de vie des ménages et profil de pauvreté à l'Extrême-Nord  
548 Cameroun en 2001. Édité. Direction de la Statistique et de la Comptabilité Nationale, étude  
549 réalisée dans la cadre du PREPAFEN, 131 p.
- 550 17. Easterling, D. R. (n.d.). Observed changes in the global distribution of daily temperature and  
551 precipitation extremes. *Climate Extremes and Society*, 24-34.  
552 doi:10.1017/cbo9780511535840.005
- 553 18. Field, C. B., Barros, V., Stocker, T. F., Dahe, Q., Dokken, D. J., Ebi, K. L., . . . Midgley, P.  
554 M. (2012). *Managing the risks of extreme events and disasters to advance climate change*  
555 *adaptation:*
- 556 19. Fischer, E. M., Beyerle, U., & Knutti, R. (2013). Robust spatially aggregated projections of  
557 climate extremes. *Nature Climate Change*, 3(12), 1033-1038. doi:10.1038/nclimate2051
- 558 20. Frédéric Saha, Mesmin Tchindjang, Jean-Guy Dzana et Djasrabé Nguemadjita, « Risques  
559 naturels dans la région de l'Extrême-Nord du Cameroun et dynamique des extrêmes  
560 hydrologiques du système Chari-Logone », *Physio-Géo*, Volume 15 | -1, 69-88.

- 561 21. Gbode, I. E., Adeyeri, O. E., Menang, K. P., Intsiful, J. D., Ajayi, V. O., Omotosho, J. A., &  
562 Akinsanola, A. A. (2019). Observed changes in climate extremes in Nigeria. *Meteorological*  
563 *Applications*, 26(4), 642-654. doi:10.1002/met.1791
- 564 22. Hamed, K. H. (2008). Trend detection in hydrologic data: the Mann–Kendall trend test under  
565 the scaling hypothesis. *Journal of hydrology*, 349(3-4), 350-363.
- 566 23. Hoeffding, W., & Kendall, M. G. (1957). Rank Correlation Methods. *Econometrica*, 25(1),  
567 181. doi:10.2307/1907752
- 568 24. Ibrahim, B., Karambiri, H., Polcher, J., Yacouba, H., & Ribstein, P. (2013). Changes in  
569 rainfall regime over Burkina Faso under the climate change conditions simulated by 5  
570 regional climate models. *Climate Dynamics*, 42(5-6), 1363-1381. doi:10.1007/s00382-013-  
571 1837-2
- 572 25. Igri, P. M., Tanessong, R. S., Vondou, D. A., Mkankam, F. K., & Panda, J. (2015). Added-  
573 Value of 3DVAR Data Assimilation in the Simulation of Heavy Rainfall Events Over West  
574 and Central Africa. *Pure and Applied Geophysics*, 172(10), 2751-2776. doi:10.1007/s00024-  
575 015-1052-7
- 576 26. Igri, P. M., Tanessong, R. S., Vondou, D. A., Panda, J., Garba, A., Mkankam, F. K., &  
577 Kamga, A. (2018). Assessing the performance of WRF model in predicting high-impact  
578 weather conditions over Central and Western Africa: An ensemble-based approach. *Natural*  
579 *Hazards*, 93(3), 1565-1587. doi :10.1007/s11069-018-3368-y
- 580 27. INS (2015) - Rapport national sur les objectifs du millénaire pour le développement en 2015.  
581 28. Édité. Institut National de la Statistique, Yaoundé (Cameroun), 48 p.
- 582 29. Iqbal, Z., Shahid, S., Ahmed, K., Ismail, T., & Nawaz, N. (2019). Spatial distribution of the  
583 trends in precipitation and precipitation extremes in the sub-Himalayan region of Pakistan.  
584 *Theoretical and Applied Climatology*, 137(3-4), 2755-2769. doi:10.1007/s00704-019-02773-  
585 4
- 586 30. Kamga, F. M. (2001). Impact of greenhouse gas induced climate change on the runoff of the  
587 Upper Benue River (Cameroon). *Journal of Hydrology*, 252(1-4), 145-156.  
588 doi:10.1016/s0022-1694(01)00445-0
- 589 31. Kharin, V. V., Zwiers, F. W., Zhang, X., & Hegerl, G. C. (2007). Changes in Temperature  
590 and Precipitation Extremes in the IPCC Ensemble of Global Coupled Model Simulations.  
591 *Journal of Climate*, 20(8), 1419-1444. doi:10.1175/jcli4066.1
- 592 32. Koutsoyiannis, D. (2003). Climate change, the Hurst phenomenon, and hydrological  
593 statistics. *Hydrological Sciences Journal*, 48(1), 3-24.
- 594 33. Leisinger, K. M., & Schmitt, K. (1995). Survival in the Sahel: An ecological and  
595 developmental challenge.

- 596 34. Leumbe, O., Bitom, D., Mamdem, L., Tiki, D., & Ibrahim, A. (2015). Cartographie des zones  
597 à risques d'inondation en zone soudano-sahélienne : cas de Maga et ses environs dans la  
598 région de l'extrême-nord Cameroun. *Afrique Science : Revue Internationale des Sciences et*  
599 *Technologie*, 11(3), 45-61.
- 600 35. Luis, M. D., González-Hidalgo, J. C., Brunetti, M., & Longares, L. A. (2011). Precipitation  
601 concentration changes in Spain 1946–2005. *Natural Hazards and Earth System Sciences*,  
602 11(5), 1259-1265. doi:10.5194/nhess-11-1259-2011
- 603 36. Mann, H. B. (1945). Nonparametric Tests Against Trend. *Econometrica*, 13(3), 245.  
604 doi:10.2307/1907187
- 605 37. McKee, T. B., Doesken, N. J., & Kleist, J. (1993, January). The relationship of drought  
606 frequency and duration to time scales. In *Proceedings of the 8th Conference on Applied*  
607 *Climatology* (Vol. 17, No. 22, pp. 179-183).
- 608 38. Min, S., Zhang, X., Zwiers, F. W., Friederichs, P., & Hense, A. (2008). Signal detectability in  
609 extreme precipitation changes assessed from twentieth century climate simulations. *Climate*  
610 *Dynamics*, 32(1), 95-111. doi :10.1007/s00382-008-0376-8
- 611 39. MINEPDED (2016) Les conditions et les stratégies de lutte contre la sécheresse au  
612 Cameroun. [https://www.droughtmanagement.info/wp-content/uploads/2016/10/WS6-](https://www.droughtmanagement.info/wp-content/uploads/2016/10/WS6-CAMEROON.pdf)  
613 [CAMEROON.pdf](https://www.droughtmanagement.info/wp-content/uploads/2016/10/WS6-CAMEROON.pdf)
- 614 40. Molua, E. L., & Lambi, C. M. (2007). The Economic Impact Of Climate Change On  
615 Agriculture In Cameroon, Volume 1of 1. *Policy Research Working Papers*.  
616 doi:10.1596/1813-9450-4364
- 617 41. Mouhamed, L., Traore, S. B., Alhassane, A., & Sarr, B. (2013). Evolution of some observed  
618 climate extremes in the West African Sahel. *Weather and Climate Extremes*, 1, 19-25. doi:  
619 10.1016/j.wace.2013.07.005
- 620 42. Neumann, J. V. (1941). Distribution of the Ratio of the Mean Square Successive Difference  
621 to the Variance. *The Annals of Mathematical Statistics*, 12(4), 367-395.  
622 doi:10.1214/aoms/1177731677
- 623 43. Niassé, M. (2004). *Reducing West Africa's vulnerability to climate impacts on water*  
624 *resources, wetlands and desertification: Elements for a regional strategy for preparedness*  
625 *and adaptation*. IUCN, Regional Office for West Africa. The World Conservation Union.
- 626 44. Nicholson, S. (2000). The nature of rainfall variability over Africa on time scales of decades  
627 to millenia. *Global and Planetary Change*, 26(1-3), 137-158. doi:10.1016/s0921-  
628 8181(00)00040-0
- 629 45. Njounwet, I., Vondou, D. A., Dassou, E. F., Ayugi, B. O., & Nouayou, R. (2021).  
630 Assessment of agricultural drought during crop-growing season in the Sudano-Sahelian

- 631 region of Cameroon. *Natural Hazards*, 106(1), 561-577.
- 632 46. Ngoma, H., Wen, W., Ayugi, B., Babaousmail, H., Karim, R., Ongoma, V. 2021c.  
633 Evaluation of rainfall simulations in CMIP6 models over Uganda. *Int. J. Climatol.*  
634 <https://doi.org/10.1002/joc.7098>
- 635 47. Oliver, J. E. (1980). Monthly Precipitation Distribution: A Comparative Index. *The*  
636 *Professional Geographer*, 32(3), 300-309. doi:10.1111/j.0033-0124.1980.00300.x
- 637 48. Penlap, E., Matulla, C., Storch, H. V., & Kanga, F. (2004). Downscaling of GCM scenarios  
638 to assess precipitation changes in the little rainy season (March-June) in Cameroon. *Climate*  
639 *Research*, 26, 85-96. doi:10.3354/cr026085
- 640 49. Pettitt, A. N. (1979). A Non-Parametric Approach to the Change-Point Problem. *Applied*  
641 *Statistics*, 28(2), 126. doi:10.2307/2346729
- 642 50. Saha, F., Tchindjang, M., Dzana, J., & Nguemadjita, D. (2020). Risques naturels dans la  
643 région de l'Extrême-Nord du Cameroun et dynamique des extrêmes hydrologiques du  
644 système Chari-Logone. *Physio-Géo*, (Volume 15), 69-88. doi:10.4000/physio-geo.10719
- 645 51. Sanogo, S., Fink, A. H., Omotosho, J. A., Ba, A., Redl, R., & Ermert, V. (2015). Spatio-  
646 temporal characteristics of the recent rainfall recovery in West Africa. *International Journal*  
647 *of Climatology*, 35(15), 4589-4605. doi:10.1002/joc.4309
- 648 52. Sultan, B., Bella-Medjo, M., Berg, A., Quirion, P., & Janicot, S. (2010). Multi-scales and  
649 multi-sites analyses of the role of rainfall in cotton yields in West Africa. *International*  
650 *Journal of Climatology: A Journal of the Royal Meteorological Society*, 30(1), 58-71.
- 651 53. Sen, P. K. (1968). Estimates of the Regression Coefficient Based on Kendall's Tau. *Journal*  
652 *of the American Statistical Association*, 63(324), 1379-1389.  
653 doi:10.1080/01621459.1968.10480934
- 654 54. Shawul, A. A., & Chakma, S. (2020). Trend of extreme precipitation indices and analysis of  
655 long-term climate variability in the Upper Awash basin, Ethiopia. *Theoretical and Applied*  
656 *Climatology*, 140(1-2), 635-652. doi:10.1007/s00704-020-03112-8
- 657 55. Shiru, M. S., Shahid, S., Chung, E. S., & Alias, N. (2019). Changing characteristics of  
658 meteorological droughts in Nigeria during 1901–2010. *Atmospheric Research*, 223, 60-73.
- 659 56. Sultan, B., Bella-Medjo, M., Berg, A., Quirion, P., & Janicot, S. (2009). Multi-scales and  
660 multi-sites analyses of the role of rainfall in cotton yields in West Africa. *International*  
661 *Journal of Climatology*. doi:10.1002/joc.1872
- 662 57. Tan, M. L., Samat, N., Chan, N. W., Lee, A. J., & Li, C. (2019). Analysis of Precipitation and  
663 Temperature Extremes over the Muda River Basin, Malaysia. *Water*, 11(2), 283.  
664 doi:10.3390/w11020283
- 665 58. Taylor, C. M., Belušić, D., Guichard, F., Parker, D. J., Vischel, T., Bock, O., . . . Panthou, G.

- 666 (2017). Frequency of extreme Sahelian storms tripled since 1982 in satellite observations.  
667 *Nature*, 544(7651), 475-478. doi:10.1038/nature22069
- 668 59. Vondou, D. A., Guenang, G. M., Djiotang, T. L. A., & Kamsu-Tamo, P. H. (2021). Trends  
669 and Interannual Variability of Extreme Rainfall Indices over Cameroon. *Sustainability*,  
670 13(12), 6803.
- 671 60. Westra, S., Alexander, L. V., & Zwiers, F. W. (2013). Global Increasing Trends in Annual  
672 Maximum Daily Precipitation. *Journal of Climate*, 26(11), 3904-3918. doi:10.1175/jcli-d-12-  
673 00502.1
- 674 61. Wijngaard, J. B., Tank, A. M., & Können, G. P. (2003). Homogeneity of 20th century  
675 European daily temperature and precipitation series. *International Journal of Climatology*,  
676 23(6), 679-692. doi:10.1002/joc.906
- 677 62. Zhang, W., Brandt, M., Tong, X., Tian, Q., & Fensholt, R. (2018). Impacts of the seasonal  
678 distribution of rainfall on vegetation productivity across the Sahel. *Biogeosciences*, 15(1),  
679 319-330.
- 680 63. Zhang, K., Yao, Y., Qian, X., & Wang, J. (2019). Various characteristics of precipitation  
681 concentration index and its cause analysis in China between 1960 and 2016. *International*  
682 *Journal of Climatology*, 39(12), 4648-4658. doi:10.1002/joc.6092.
- 683 64. Zhang L, Qian Y (2003). Annual distribution features of precipitation in China and their  
684 interannual variations. *Acta Meteorological Sinica* 17(2): 146–163.

685

686

687

688

689

690 **Table 1** Geographical descriptions of the data, altitude, period of measurement and percentage of  
691 missing data.

N°	Stations	Latitude(°N)	Longitude(°E)	Altitude(m)	Period	Missing(%)
1	Bidzar	9.9	14.12	470	1980-2019	1.8
2	Fignole	8.57	13.05	523	1980-2019	0
3	Guetale	10.07	13.91	490	1980-2019	2.8
4	Guider	9.03	13.95	356	1980-2019	2.8
5	Guidiguis	10.10	14.71	362	1980-2019	0.8
6	Hina-marbak	10.37	13.85	544	1980-2019	0.8
7	Kaélé	10.08	14.43	388	1980-2019	0
8	Pitoe	9.34	13.53	274	1980-2019	0
9	Tchatibili	10.05	14.91	815	1980-2019	0
10	Touboro	7.67	15.37	500	1980-2019	0.6
11	Yagoua	10.35	15.23	325	1980-2019	0
12	Bere	9.01	14.23	238	1980-2018	0
13	Garoua	8.56	13.05	213	1980-2018	0.8
14	Madingring	8.45	15.00	430	1980-2018	0
15	Tchollire	8.4	14.16	392	1980-2018	1.7
16	Maroua	10.58	14.30	428	1980-2015	0
17	Doukoula	10.12	14.97	340	1980-2012	3
18	Gawar	10.51	13.85	420	1980-2012	0.4
19	Lara	10.17	14.51	416	1980-2012	0.4
20	Mokolo	10.73	13.82	795	1980-2012	0
21	Mora	11.05	14.15	438	1980-2012	0

22	Ndock	7.96	14.67	489	1980-2012	0
23	Sanguere	9.08	13.52	418	1980-2012	0
24	Waza	11.40	14.57	311	1980-2012	0
25	Soudounkou	9.85	13.88	358	1980-2011	0

692

693 **Table 2** Definition of ETCCDI indices based on daily precipitation and units.

Variables	Description	Definitions	Units
cdd	Consecutive dry days	Maximum number of consecutive dry days	days
cwd	Consecutive wet days	Maximum number of consecutive wet days	days
r10	Number of heavy precipitation days	Annual count of days when $RR \geq 10$ mm	Days
r20	Number of very heavy precipitation days	Annual count of days when $RR \geq 20$ mm	Days
r25	Number of very heavy precipitation days	Annual count of days when $RR \geq 25$ mm	Days
ptot	Annual precipitation	Annual total precipitation when $RR \geq 1$ mm	mm
r95p	Very wet days	Annual total precipitation when $RR >$ 95th percentile	mm
r99p	Extremely wet days	Annual total precipitation when $RR >$ 99th percentile	mm
rx1day	Maximum 1 day precipitation	Annual highest daily precipitation	mm

rx5day	Maximum 5-day precipitation	Annual highest 5 consecutive days precipitation	mm
sdi	Simple daily intensity index	Annual precipitation divided by number of wet days	mm/day

694

695

696 **Table 3** Statistical test of homogeneity applied to the annual rainfall count series of main climate  
697 stations in the sudano-sahelian region of Cameroon.

N°	Stations	SNHT	Pettitt's test	Buishand's test	Von Neumann's test	decision
1	Bidzar	36	8	30	1.74	Useful
2	Fignole	38*	30*	30*	1.58	Doubtful
3	Guetale	39*	11	11	1.40*	Doubtful
4	Guider	36*	27	27	1.70	Useful
5	Guidiguis	6	6	6	2.06	Useful
6	Hina-marbak	39*	13	32	1.40*	Doubtful
7	Kaélé	38*	11	11	1.31	Useful
8	Pitoea	31*	31	31	1.37	Useful
9	Tchatibili	6	14	11	1.56	Useful
10	Touboro	10*	15*	15*	1.96	Doubtful
11	Yagoua	38	14	36	1.78	Useful
12	Bere	17	17	17	1.32	Useful
13	Garoua	8	31	8	1.68	Useful

14	Madingring	31	31	23*	1.57	Useful
15	Tchollire	8	8	8	1.97	Useful
16	Maroua	23*	23*	23	1.53	Doubtful
17	Doukoula	14	14	14	1.89	Useful
18	<b>Gawar</b>	<b>23*</b>	<b>23*</b>	<b>23*</b>	<b>1.61</b>	<b>Suspect</b>
19	Lara	8	8	8	1.76	Useful
20	Mokolo	20	10	20	2.11	Useful
21	<b>Mora</b>	<b>11*</b>	<b>11*</b>	<b>11*</b>	<b>1.19</b>	<b>Suspect</b>
22	Ndock	23	23	23*	1.70	Useful
23	Sanguere	21	21	21	1.73	Useful
24	Waza	11	11*	11	1.79	Useful
25	Soudoukou	30	12	22	2.00	Useful

698 (\*) indicate that the test rejects the null hypothesis at the 1% level and the annual data series is

699 not homogenous

700 **Table 4** Summary (minimum, maximum and natural variability) and Modified Mann-Kendall trend  
701 statistics for total annual precipitation. Significant changes (i.e. Z greater than 1.96) are indicated in  
702 bold. The abbreviations are NT = no trend, P = positive trend, SP = significant positive trend, N =  
703 negative trend, and SN = significant negative trend.

704

Stations	Annual Max (mm)	Annual (mm)	Min	Standard deviation	Z-statistics	Sen's slope (mm)	Trend
Bidzar	1319	534.9		183.5	0.36	1	P
Figrole	1654	688		221.6	-0.46	-3.0	N

Guetale	1013	436	135.2	1.39	5.16	P
Guider	1212	557	171.9	-0.54	-1.53	N
Guidiguis	1077	597	138.2	1.08	2.58	P
Hina-marbak	1260	554.2	168.1	<b>2.25</b>	<b>7.04</b>	<b>SP</b>
Kaélé	1080	604.7	151.7	<b>2.27</b>	<b>6.34</b>	<b>SP</b>
Pitoa	1304	387	182.2	0.45	6.22	P
Tchatibili	1162	491	169.1	0.70	2.18	P
Touboro	1539	830	195.9	0.91	9.47	P
Yagoua	1044	110	170.3	1.05	1.40	P
Bere	1258	554	176.3	<b>2.58</b>	<b>3.52</b>	<b>SP</b>
Garoua	1258	554	194.8	<b>2.48</b>	<b>3.82</b>	<b>SP</b>
Madingring	1336	660	170.1	1.05	3.15	P
Tchollire	1670	736	208.9	<b>2.59</b>	<b>10</b>	<b>SP</b>
Maroua	1333	530.1	218.6	<b>2.48</b>	<b>10</b>	<b>SP</b>
Doukoula	1162	491	179.3	1.16	4	P
Lara	1244	462	162	1.08	2.62	P
Mokolo	1458	721.7	172.8	1.42	3.46	P
Ndock	1708	845	225.8	-0.33	-1.23	N
Sanguere	1393	670	161.8	-1.04	-3.88	N
Waza	954.6	441.8	115.2	1.61	2.67	P
Soudoukou	1575	561	202.2	-0.18	-0.68	N

706 **Table 5** Correlation coefficients of annual extreme precipitation indices for baseline precipitation  
 707 data from 1980 to 2012 in the sub-humid region of Cameroon.

708

Indices	CDD	CWD	PTOT	R10	R20	R25	R95p	R99p	Rx1day	Rx5day	SDII
CDD	1*										
CWD	-0.33	1*									
PTOT	-0.35	0.40*	1*								
R10	-0.47	0.34*	0.94*	1*							
R20	-0.23	0.28	0.92*	0.83*	1*						
R25	-0.12	0.24	0.88*	0.77*	0.95*	1*					
R95p	-0.09	0.45*	0.74*	0.56*	0.68*	0.71*	1*				
R99p	0.01	0.37*	0.62*	0.45*	0.45*	0.49*	0.85*	1*			
Rx1day	0.01	0.31*	0.58*	0.39*	0.41*	0.47*	0.80*	0.91*	1*		
Rx5day	0.01	0.42*	0.64*	0.49*	0.56*	0.59*	0.82*	0.75*	0.81*	1*	
SDII	0.23	0.02	0.30*	0.13	0.42*	0.53*	0.65*	0.46*	0.43*	0.52*	1*

709 (\*) significant at the 95% confidence level

710

711

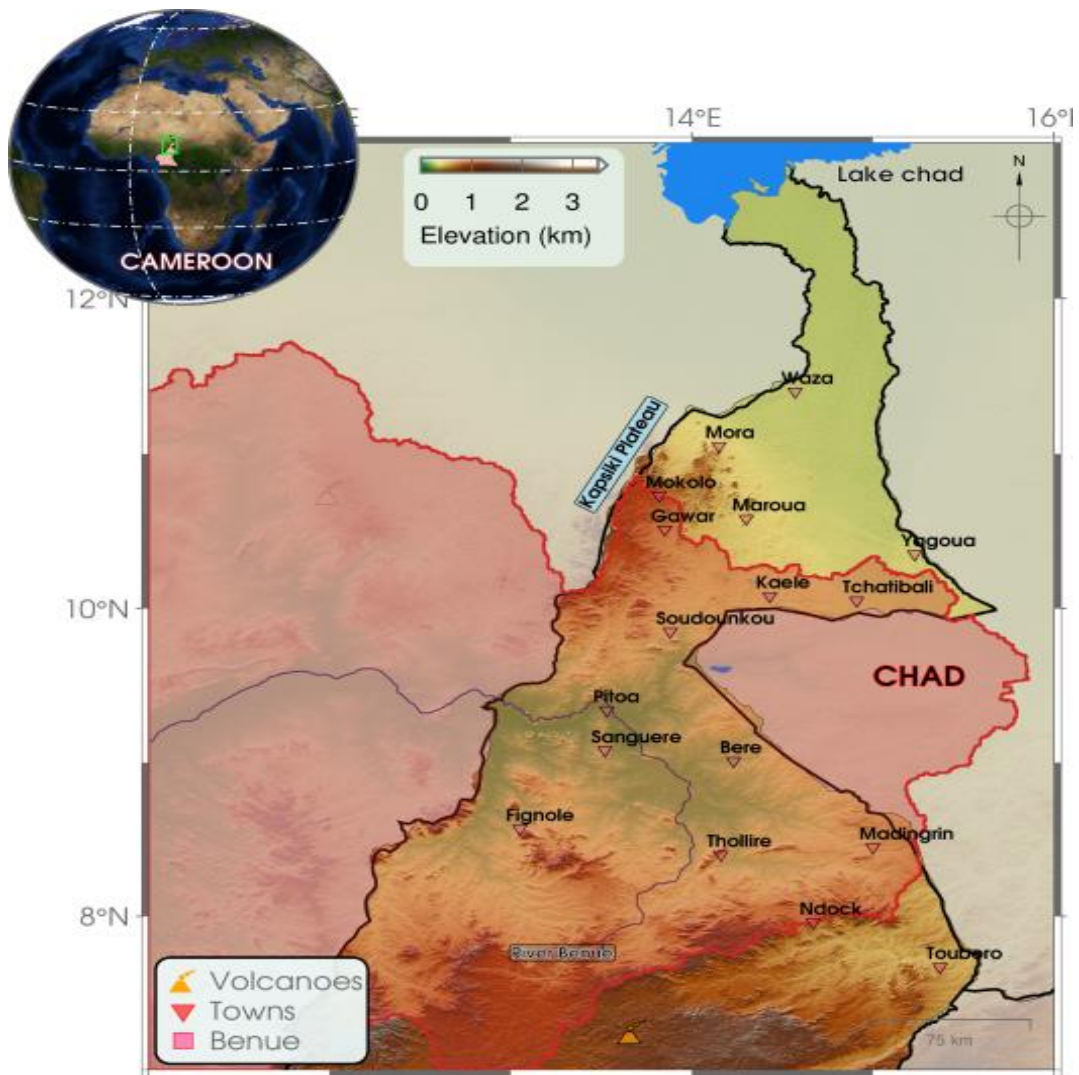


**Fig. 1** Map of the study area with the Sudano-Sahelian political border of Cameroon, topography and selected rainfall stations. Red line delineates the water catchment boundary.

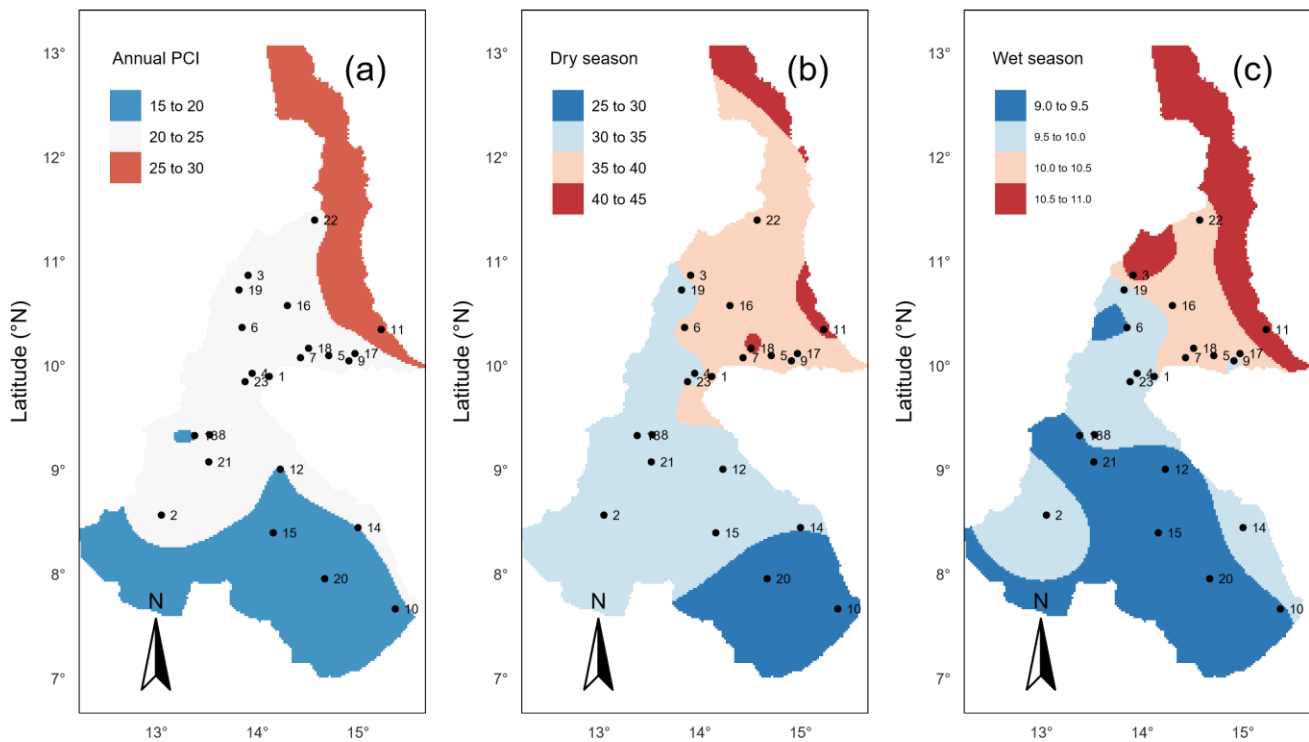
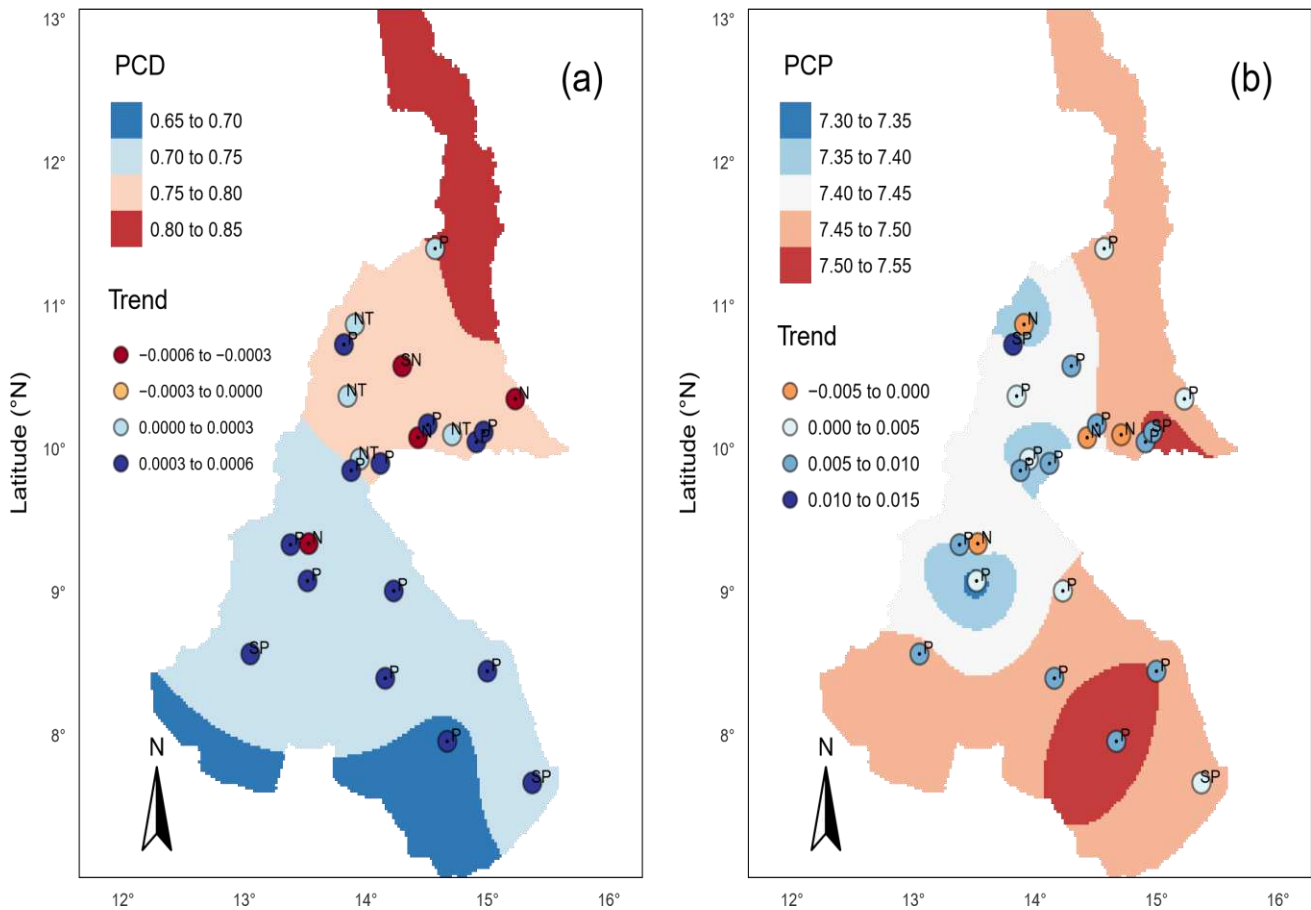


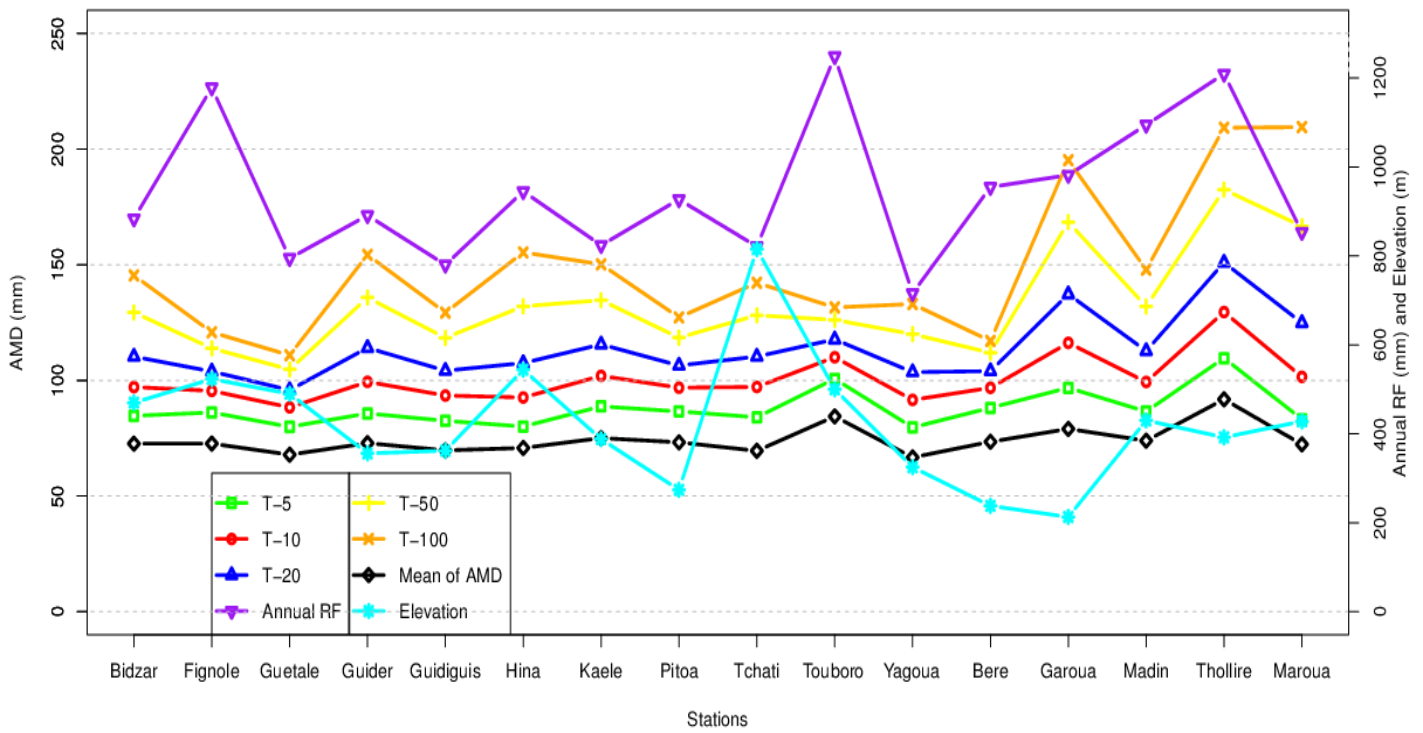
**Fig. 2** Spatial map of mean value of (a) annual precipitation concentration index (PCI), (b) dry season PCI, and (c) rainy season PCI over in the Sudano-Sahelian region of Cameroon.

754  
755  
756  
757  
758



759  
760  
761  
762  
763  
764  
765  
766  
767  
768

**Fig. 3** Spatial distribution of mean annual values and trends for variability parameters from 1980 to 2012 **a** Precipitation Concentration Degree (PCD), and **b** Precipitation Concentration Period (PCP). The abbreviations are NT = no trend, P = positive trend, SP = significant positive trend, N = negative trend, and SN = significant negative trend.



769

770

771

772

773

774

775

776

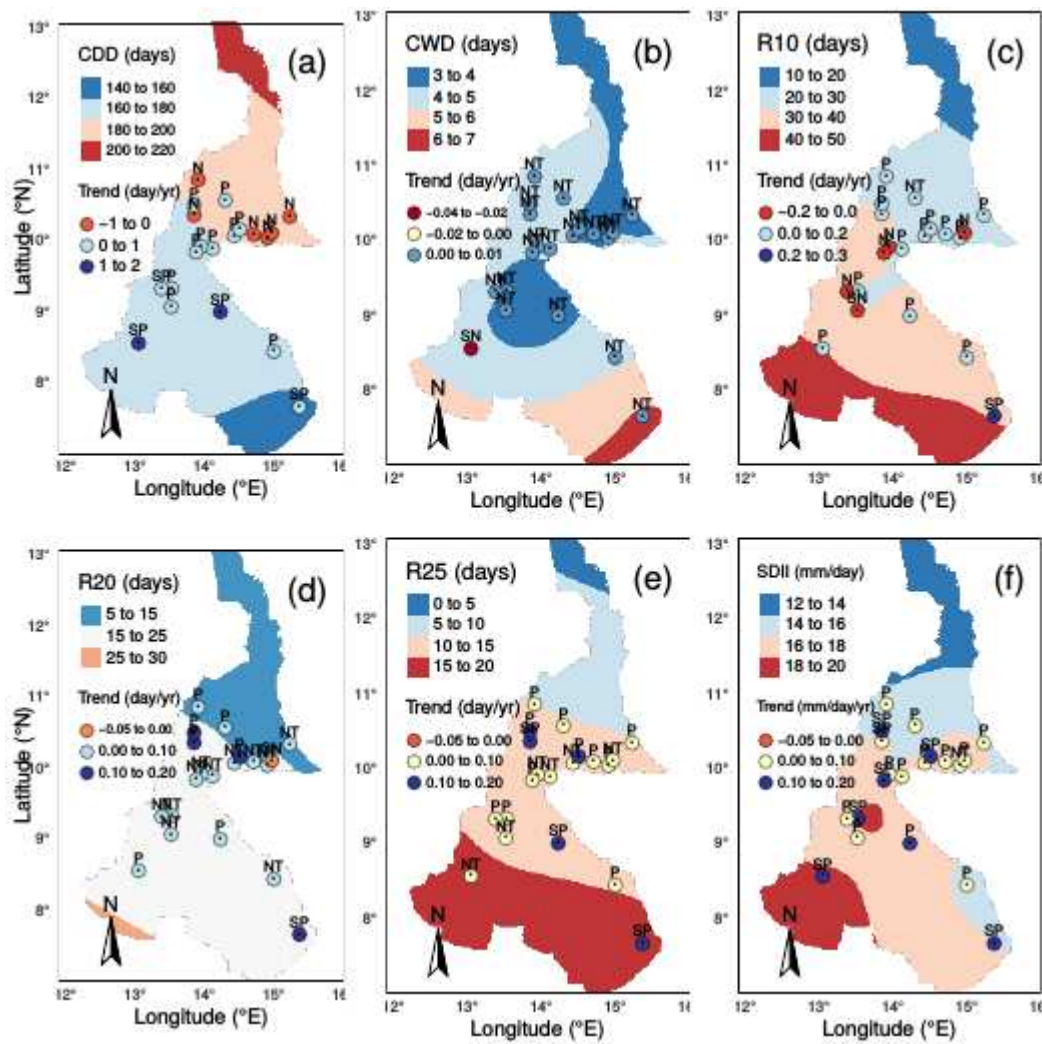
777

778

779

780

**Fig. 4** Annual maximum daily (AMD) rainfall (mm) for different return periods in year (T-100yr, T-50yr, T-20yr, T-10yr, and T-5yr), mean of AMD rainfall and precipitation, and elevation for baseline precipitation data from 1980 to 2019.



781

782

783 **Fig. 5** Spatial distribution of average and trends for extreme precipitation indices from 1980 to 2012

784 (a) CDD, (b) CWD, (c) R10, (d) R20, (e) R25, and (f) SDII. The abbreviations are NT = no trend, P

785 = positive trend, SP = significant positive trend, N = negative trend, and SN = significant negative

786 trend.

787

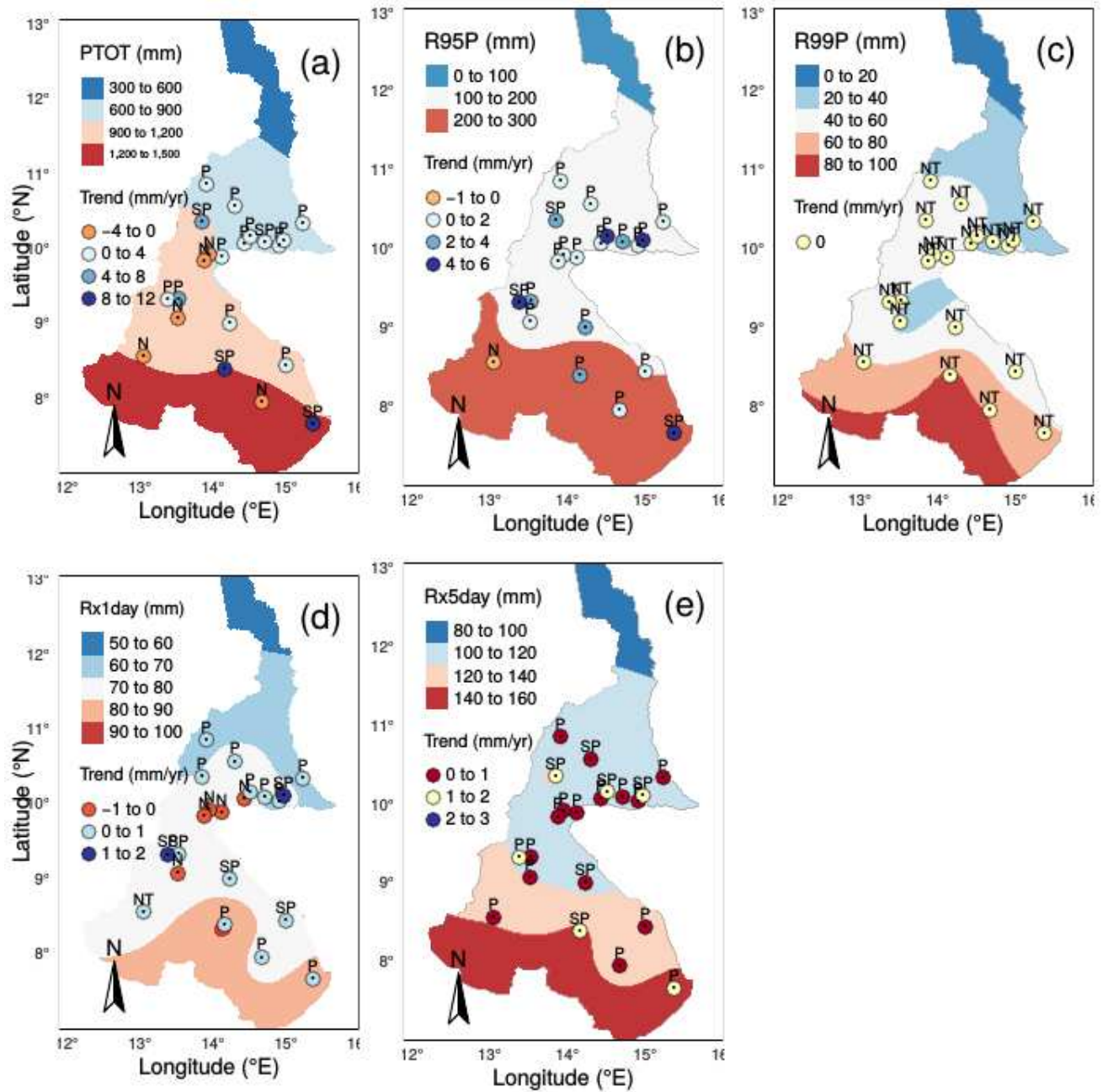
788

789

790

791

792



793

794

795 **Fig. 6** Spatial distribution of average annual values and trends for extreme precipitation

796 amount/intensity/days indices from 1980 to 2012 (a) PTOT, (b) R95p, (c) R99p, (d) Rx1day, and (e)

797 Rx5day.

798

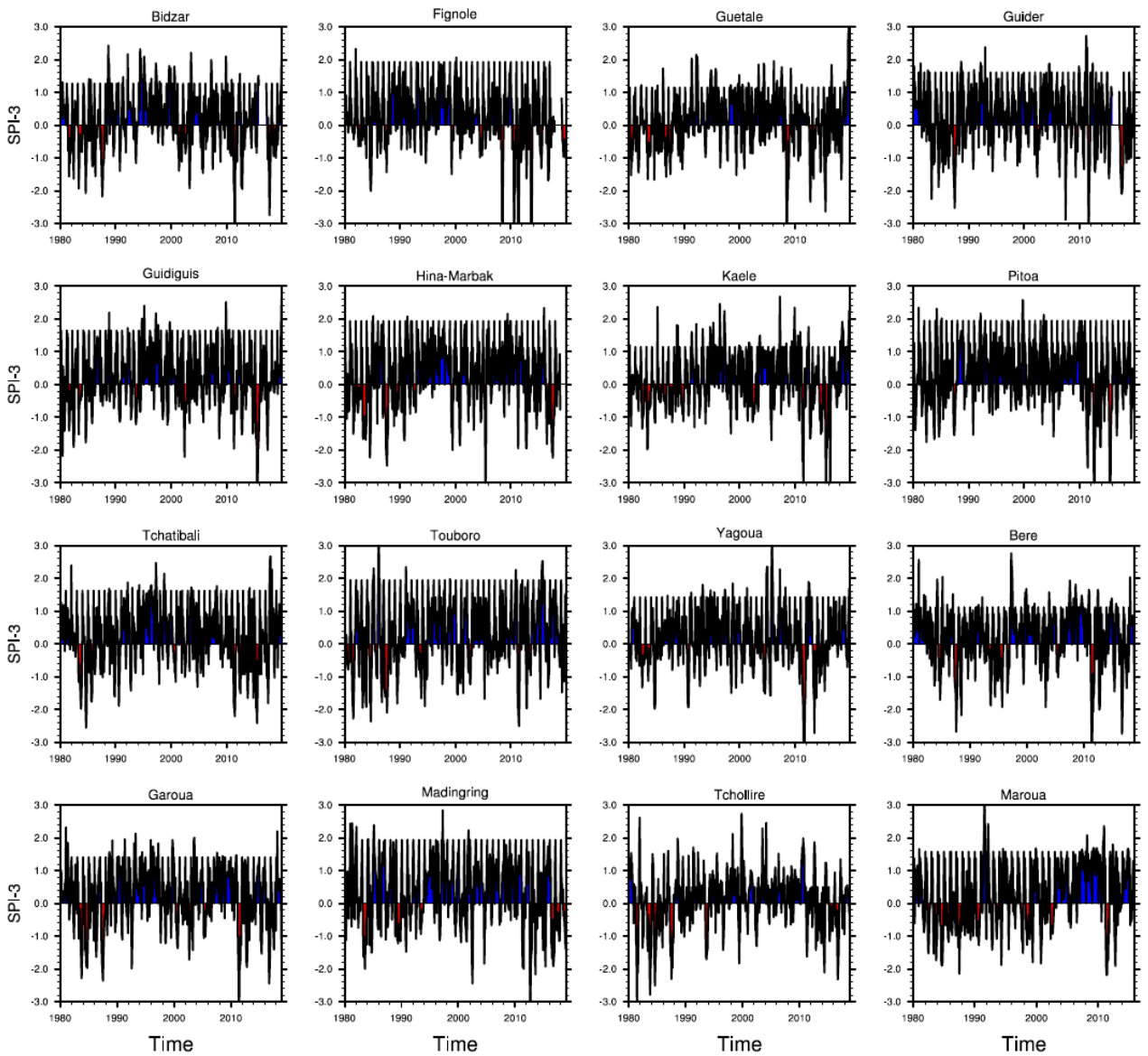
799

800

801

802

803



804  
 805  
 806  
 807  
 808  
 809

**Fig. 7** The 3-month-scale Standardized precipitation index (SPI) time series for selected stations from 1980 to 2019 in the Sudano-Sahelian region of Cameroon for wet conditions (blue) and drought conditions (red).

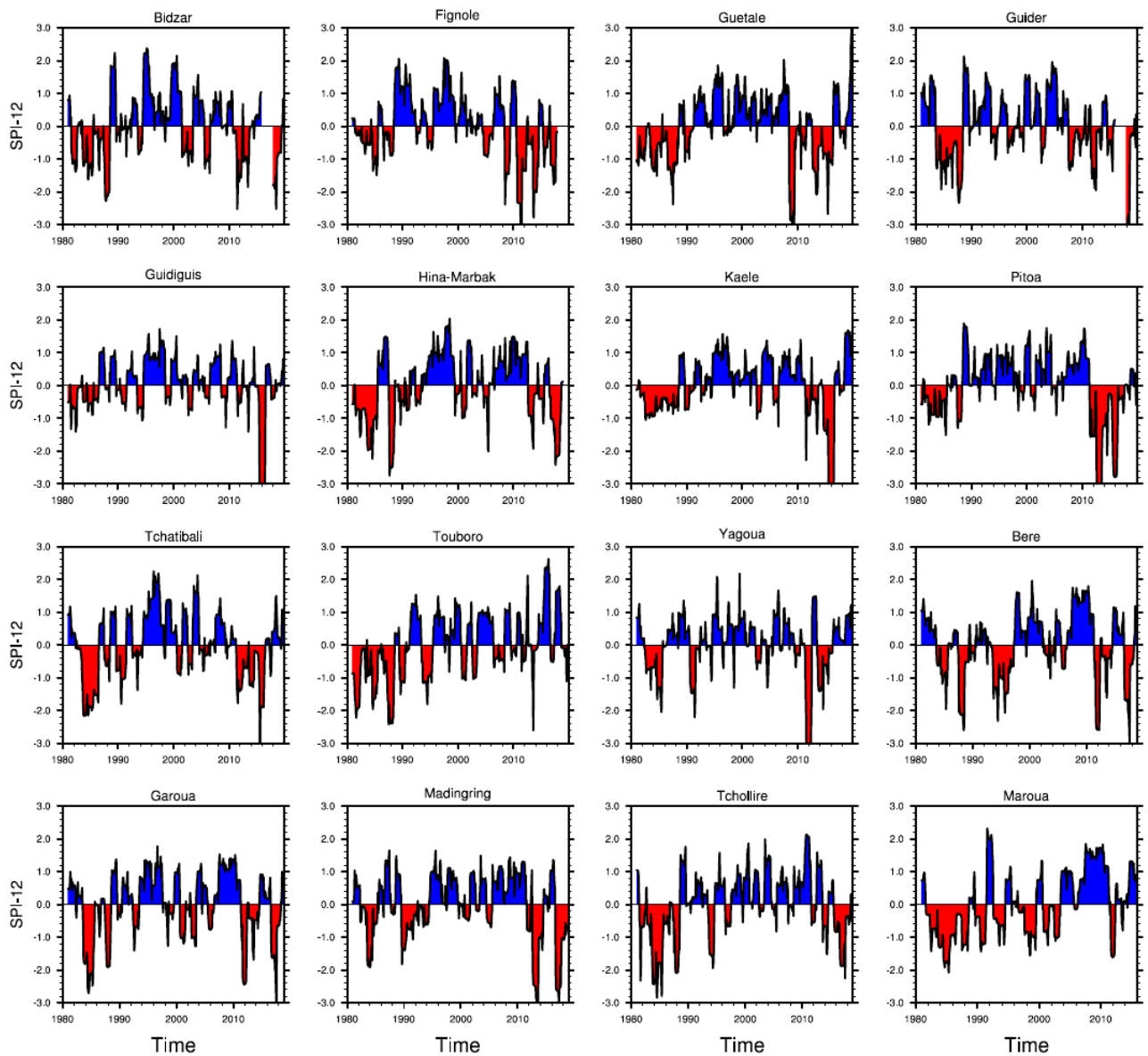


**Fig. 8** The 12-month-scale Standardized precipitation index (SPI) time series for selected stations from 1980 to 2019 in the Sudano-Sahelian region of Cameroon for wet conditions (blue) and drought conditions (red).

810  
811  
812  
813  
814